NEVITT, M. V. (1963). In *Electronic Structure and Alloy Chemistry of the Transition Elements*. Ed. P. Beck, New York: Interscience, John Wiley.
NOWOTNY, H. & AUER-WELSBACH, H. (1961). *Mh. Chem.* **92**, 789.
PARTHÉ, E. (1959). *Acta Cryst.* **12**, 559.
PARTHÉ, E. (1961). *Z. Kristallogr.* **115**, 52. (In Fig. 6 are compared space-filling curves for FeSi (*B*20), FeB (*B*27), CrB (*B*33) and NaCl (*B*1) structure types. The curve for the CsCl (*B*1) structure type is very similar to the curve for FeSi type with discontinuity points at the same ε values of 0·731 and 1·365, however, altogether vertically shifted to slightly higher space-filling values.)
PARTHÉ, ERWIN & PARTHÉ, EDDA. (1963). *Acta Cryst.* **16**, 71.
PARTHÉ, E., HOHNKE, D., JEITSCHKO, W. & SCHOB, O. (1965). *Naturwissenschaften*, **52**, 155.
PÖTZSCHKE, M. & SCHUBERT, K. (1962). *Z. Metallk.* **53**, 548.
PRZYBYLSKA, M., REDDOCH, A. H. & RITTER, G. J. (1963). *J. Amer. Chem. Soc.* **85**, 407.
ROCKTAESCHEL, R. & WEISS, A. (1962). *Z. anorg. Chem.* **316**, 261.
SANDS, D. E., WOOD, D. H. & RAMSEY, W. J. (1964). *Acta Cryst.* **17**, 986.
SCHOB, O., NOWOTNY, H. & BENESOVSKY, F. (1961). *Mh. Chem.* **92**, 1218.
SCHOB, O. & PARTHÉ, E. (1964). *Mh. Chem.* **95**, 1466.
SPEDDING, F. H. & DAANE, A. H. (1961). *The Rare Earths.* New York: John Wiley.
SPEDDING, F. H., VALLETTA, R. M. & DAANE, A. H. (1962). *Amer. Soc. Met. Trans.* **55**, 483.
SPOONER, F. J. & WILSON, C. G. (1962). *Acta Cryst.* **15**, 621.
THOMSON, J. R. (1962*a*). *Nature, Lond.* **194**, 465.
THOMSON, J. R. (1962*b*). *Acta Cryst.* **15**, 1308.
WABER, J. T., GSCHNEIDNER, K., LARSON, A. C. & PRINCE, M. Y. (1963). *Trans. Amer. Inst. Min. (metall.) Engrs.* **227**, 717.
ZHURAVLEV, N. N. & SMIRNOVA, E. M. (1962). *Soviet Phys. Cryst.* **7**, 243.

Acta Cryst. (1965). **19**, 224

Comparison of Scattering Factors Computed from Four Different Atomic Models*

BY DON T. CROMER

University of California, Los Alamos Scientific Laboratory, Los Alamos, New Mexico, U.S.A.

(*Received* 3 *November* 1964)

Scattering factors computed from four different atomic models are compared at various values of sin θ/λ throughout most of the Periodic Table. The differences are discussed in relation to the differences in the atomic models.

Introduction

Scattering factors calculated from four different atomic models are now available for nearly all atoms. These models are the Thomas–Fermi–Dirac (TFD), which is the familiar statistical model including exchange; the non-relativistic Hartree (H) without exchange (Cromer, Larson & Waber, 1963, 1964); the Hartree–Fock–Slater (HFS), similar to Hartree but including Slater's approximate exchange correction (Hanson, Herman, Lea & Skillman, 1964); and the Dirac–Slater (DS), the relativistic equivalent of the HFS model (Cromer & Waber, 1964, 1965).

Differences between these scattering factors have been plotted *versus Z* (atomic number) for various values of sin θ/λ. These differences are briefly discussed in relation to the differences in the atomic models. A large number of sets of differences were initially calculated and plotted with the use of a computer. The various scattering curves were fitted to analytic functions to facilitate entry of all the information into the computer. A representative few have been selected for the present discussion.

As a general rule, differences in scattering factors at low values of sin θ/λ arise because of differences in

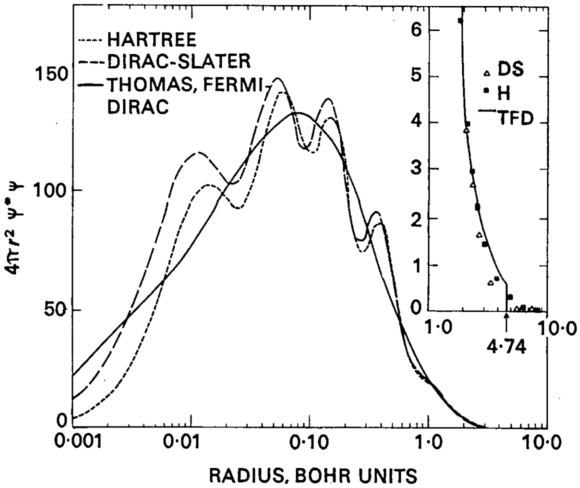

Fig. 1. Radial electron density plots for three different models of the Hg atom. The inset shows the details at large radii.

---

* Work performed under the auspices of the U.S. Atomic Energy Commission.

the outer or valence electrons, while at large values of $\sin\theta/\lambda$ the differences in the core electron distributions produce the differences in scattering factors.

The charge distribution for Hg, a typical heavy atom, as computed from three of the four atomic models is shown in Fig. 1. The TFD curve was computed by Abrahamson (1961), the H curve by Boyd, Larson and Waber (1963) and the DS curve by Liberman, Waber & Cromer (1965). The HFS distribution would be similar to the DS but slightly expanded.

Discussion

The difference between the TFD and the H scattering factors has already been discussed by Cromer, Larson & Waber (1964). They showed that at small $\sin\theta/\lambda$ the difference $(f_{\mathrm{TFD}}-f_{\mathrm{H}})$ should always be positive because the TFD electron density is normalized by an abrupt drop to zero at a certain radius r_{D}. The difference $(f_{\mathrm{TFD}}-f_{\mathrm{H}})$ is then related to the number of electrons in the Hartree density that lie at a radius greater than r_{D}.

According to the above reasoning, at small enough $\sin\theta/\lambda$, f_{TFD} should be larger than any other f computed from an electron density distribution that approaches zero at a radius larger than r_{D}. In Fig. 2 the difference $(f_{\mathrm{TFD}}-f_{\mathrm{DS}})$ is plotted *versus* Z at $\sin\theta/\lambda=0{\cdot}05$ and $0{\cdot}01$ Å^{-1}. Because the DS atom is more compact than the Hartree atom there is a much smaller number of electrons outside r_{D}. Therefore f_{TFD} is not always greater than f_{DS} until $\sin\theta/\lambda$ is as small as about 0·01.

The difference $(f_{\mathrm{TFD}}-f_{\mathrm{HS}})$ is very similar at small $\sin\theta/\lambda$ to $(f_{\mathrm{TFD}}-f_{\mathrm{DS}})$ as given in Fig. 2. It follows that for small $\sin\theta/\lambda$ $(f_{\mathrm{HFS}}-f_{\mathrm{DS}})$ is small. This difference, at $\sin\theta/\lambda=0{\cdot}03$, is given in Fig. 3. The HFS and DS atomic models differ only in that DS is relativistic, and relativistic effects are small for the outer electrons. Differences in scattering curves at small $\sin\theta/\lambda$ reflect differences in the outer region of the atoms. At very high atomic numbers a relativistic contraction of the outer electrons does occur and thus the curve of Fig. 3 becomes slightly negative.

Fig. 4 shows $(f_{\mathrm{TFD}}-f_{\mathrm{HFS}})$ at $\sin\theta/\lambda=0{\cdot}05$. The difference is no longer uniformly positive or negative.

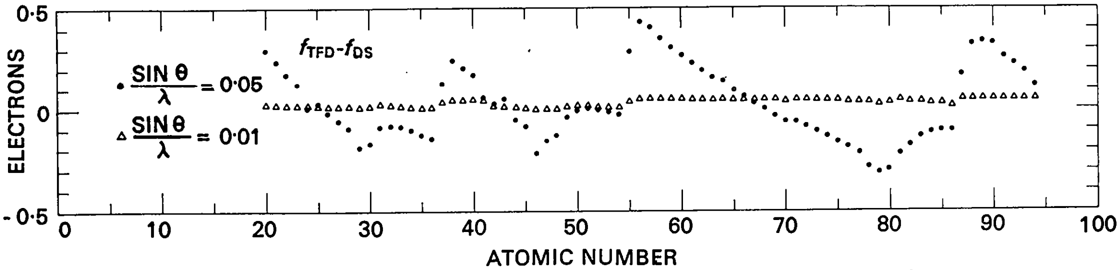

Fig. 2. $(f_{\mathrm{TFD}}-f_{\mathrm{DS}})$ plotted *vs* atomic number at $\sin\theta/\lambda=0{\cdot}01$ and $0{\cdot}05$ Å^{-1}.

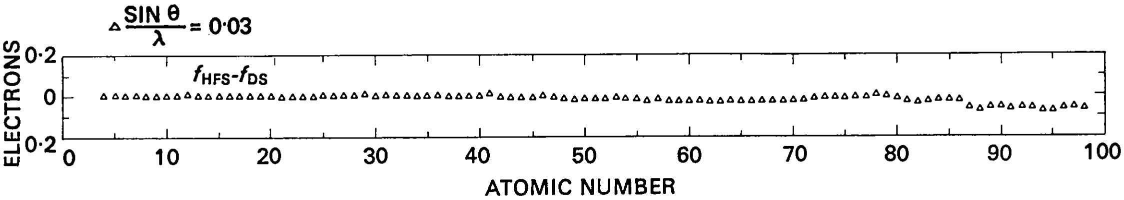

Fig. 3. $(f_{\mathrm{HFS}}-f_{\mathrm{DS}})$ plotted *vs* atomic number at $\sin\theta/\lambda=0{\cdot}03$ Å^{-1}.

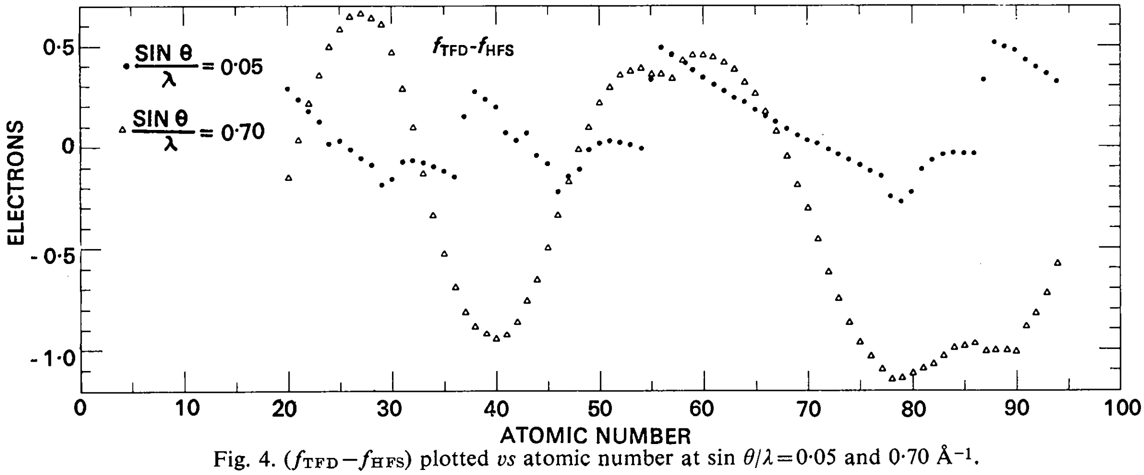

Fig. 4. $(f_{\mathrm{TFD}}-f_{\mathrm{HFS}})$ plotted *vs* atomic number at $\sin\theta/\lambda=0{\cdot}05$ and $0{\cdot}70$ Å^{-1}.

Both of these atomic models are non-relativistic and both account approximately for exchange. However, the TFD model has a smooth radial electron density distribution with a single broad maximum while the HFS model has a shell structure. The differences in these two scattering factors must therefore be primarily due to the shell structure. There are minima at each of the rare gases. The curves rise sharply with the start of a new shell of electrons after the rare gases and then fall until the shell is filled. In a TFD atom the *s* electron added after a rare gas is no different from the other electrons, but in any of the other models a new shell is started and the extra *s* electron is considerably removed from the rest, as noted by Waber & Cromer (1965) in a paper on orbital radii. There are other discontinuities in this curve besides those at the filled shells. These are related to discontinuities of configuration. For example, the dip at Cr, $Z=24$, reflects the fact that Cr has only one 4*s* electron in the ground state whereas V, $Z=23$, and Mn, $Z=25$, each have two 4*s* electrons. The difference $(f_{\text{TFD}}-f_{\text{HFS}})$ at $\sin\theta/\lambda=0{\cdot}70$ is also plotted in Fig. 4. Any discontinuities because of configuration changes are smoothed out. These changes affect only the outer electrons and all detail of these electrons is lost at large $\sin\theta/\lambda$. Only two broad minima remain. These occur approximately where the 4*d* shell and the 4*f* shell have been filled. In these regions of the periodic table the HFS atom, with a shell structure, has larger local densities than the statistical TFD atom.

In Fig. 5, the difference $(f_{\text{H}}-f_{\text{HFS}})$ is plotted for $\sin\theta/\lambda=0{\cdot}05$, $0{\cdot}20$ and $0{\cdot}70$ Å^{-1}. This difference is always negative and at times is as large as $-1{\cdot}5$ electrons. These two models differ only because exchange has been approximately accounted for in the HFS model. Both models have the same shell structure and extend, in principle, to infinity. However, the electrons are more tightly bound in the HFS model because of the exchange potential. Configurational discontinuities are again apparent but these are smoothed out at large $\sin\theta/\lambda$, as expected.

In Fig. 6 the difference $(f_{\text{H}}-f_{\text{DS}})$ is plotted at $\sin\theta/\lambda=0{\cdot}05$, $0{\cdot}20$ and $0{\cdot}70$ Å^{-1}. These differences are always negative, as in Fig. 5, but the differences are generally larger. In the DS model there is a contraction not only because of exchange but also because of relativistic effects.

In Fig. 7 the HFS and DS models are compared. The difference $(f_{\text{HFS}}-f_{\text{DS}})$ is plotted at $\sin\theta/\lambda=0{\cdot}20$ and $0{\cdot}70$ Å^{-1}. The difference at $\sin\theta/\lambda=0{\cdot}03$ has already been given in Fig. 3. At low atomic number these two models should give identical results because relativity

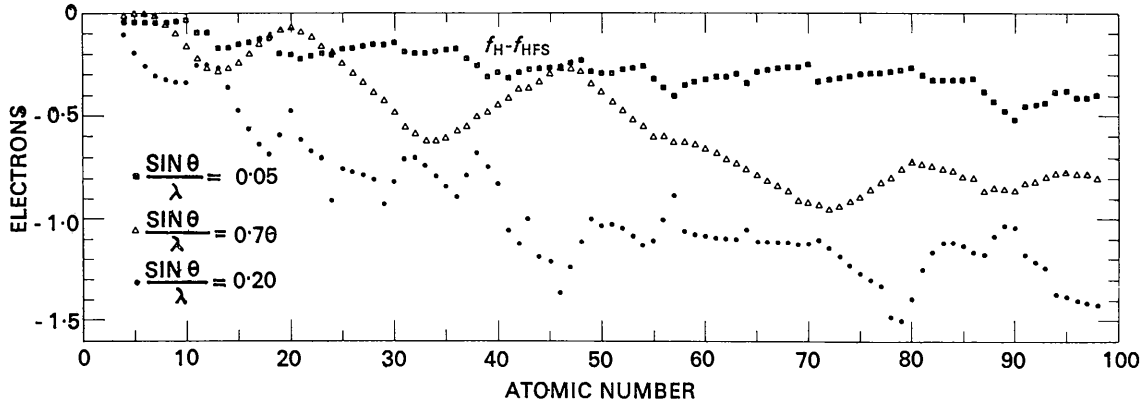

Fig. 5. $(f_{\text{H}}-f_{\text{HFS}})$ plotted *vs* atomic number at $\sin\theta/\lambda=0{\cdot}05$, $0{\cdot}20$ and $0{\cdot}70$ Å^{-1}.

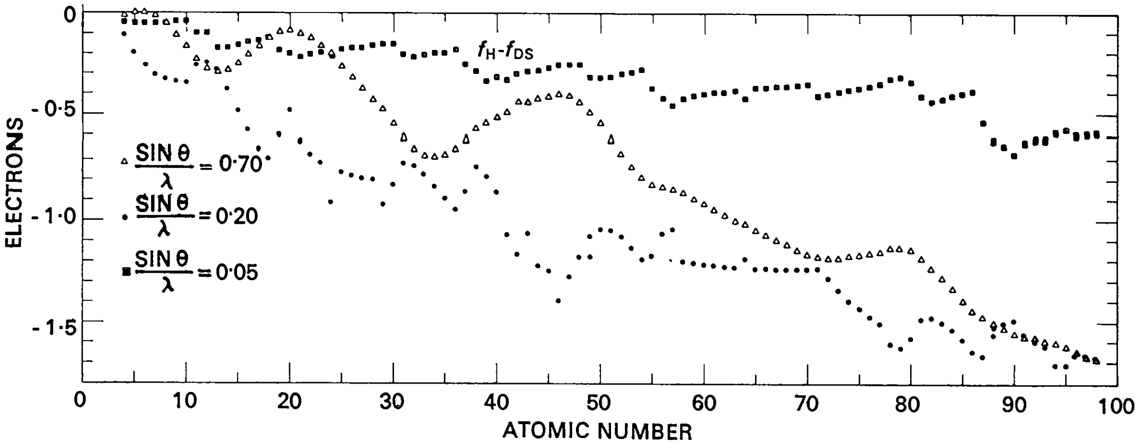

Fig. 6. $(f_{\text{H}}-f_{\text{DS}})$ plotted *vs* atomic number at $\sin\theta/\lambda=0{\cdot}05$, $0{\cdot}20$ and $0{\cdot}70$ Å^{-1}.

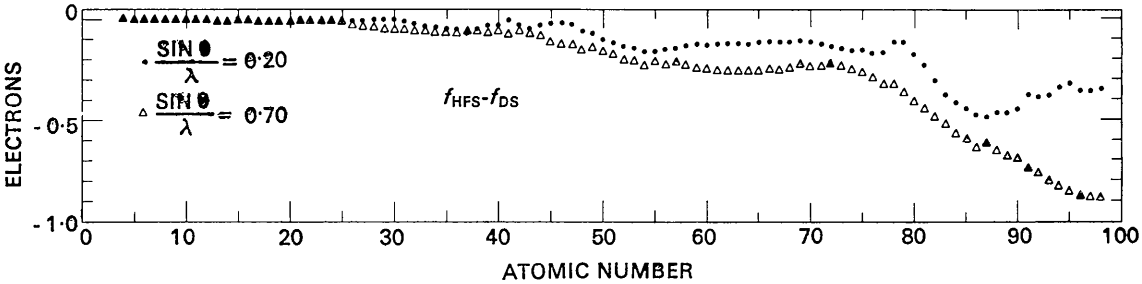

Fig. 7. ($f_{HFS}-f_{DS}$) plotted *vs* atomic number at $\sin\theta/\lambda = 0{\cdot}20$ and $0{\cdot}70$ Å^{-1}.

effects are negligible and these two models differ only in this respect. The differences are essentially zero. (The small deviation from zero of the plotted differences at low atomic number arises for the most part from small inaccuracies in the analytic fits used to compute the differences). At the higher atomic numbers the difference is always negative because the relativistic DS atomic model is more compact than the nonrelativistic HFS model.

As a general rule, the inclusion of exchange has a greater effect on the scattering factors than does relativity. At the heaviest elements the two effects appear to be comparable.

Conclusions

Crystallographers now are overwhelmed with scattering factors and one might well ask which of these he should use. For the lighter elements, up to Rb$^+$, the values given in *International Tables for X-ray Crystallography* (1962) are the best ones, for they have been computed from Hartree–Fock wave functions and in some cases from even more accurate wave functions. For these lighter elements, relativistic effects are trivial. For heavier elements it is suggested that the Dirac–Slater scattering factors are to be preferred because relativistic effects are accounted for and at least an approximation for exchange has been made.

References

Abrahamson, A. A. (1961). *Phys. Rev.* **123**, 538.

Boyd, R. G., Larson, A. C. & Waber, J. T. (1963). To be published.

Cromer, D. T., Larson, A. C. & Waber, J. T. (1963). Los Alamos Scientific Laboratory Report, LASL-2987.

Cromer, D. T., Larson, A. C. & Waber, J. T. (1964). *Acta Cryst.* **17**, 1044.

Cromer, D. T. & Waber, J. T. (1964). Los Alamos Scientific Laboratory Report, LASL-3056.

Cromer, D. T. & Waber, J. T. (1965). *Acta Cryst.* **18**, 104.

Hanson, H. P., Herman, F., Lea, J. D. & Skillman, S. (1964). *Acta Cryst.* **17**, 1040.

International Tables for X-ray Crystallography (1962). Vol. III. Birmingham: Kynoch Press.

Liberman, D., Waber, J. T. & Cromer, D. T. (1965). *Phys. Rev.* **137**, A 27.

Waber, J. T. & Cromer, D. T. (1965). *J. Chem. Phys.* In the press.

Acta Cryst. (1965). **19**, 227

The Crystal Structure of [18]annulene. I. X-ray Study

By Judith Bregman*, F. L. Hirshfeld, D. Rabinovich and G. M. J. Schmidt
Department of X-ray Crystallography, Weizmann Institute of Science, Rehovoth, Israel

(*Received* 29 *October* 1964 *and in revised form* 8 *January* 1965)

The crystal structure of [18] annulene has been determined by least-squares analysis of photographic X-ray data recorded at the temperature of boiling nitrogen. The molecules occupy crystallographic centers of symmetry in a structure closely resembling that of coronene. This molecular symmetry rules out the possibility of a structure with alternate long and short C–C bonds. Final carbon coordinates have estimated standard deviations averaging less than 0·004 Å; the hydrogen atoms have not been reliably located.

Introduction

The synthesis by Sondheimer and his collaborators (Sondheimer & Wolovsky, 1959; Sondheimer & Gaoni, 1960, 1961, 1962; Sondheimer, Wolovsky & Gaoni, 1960; Sondheimer, Wolovsky & Amiel, 1962; Sondheimer, 1963) of the monocyclic alternant hydrocarbons C_nH_n ($n = 14,16,18,20,24,30$) has made available a class of compounds ('annulenes') of considerable

---

* Present address: Department of Physics, Polytechnic Institute of Brooklyn, Brooklyn 1, N.Y., U.S.A.